Journal of Materials Chemistry A

Accepted Manuscript

ROYAL SOCIETY OF CHEMISTRY

www.rsc.org/materialsA

Journal Name

RSCPublishing

COMMUNICATION

Copper Phosphide Modified Cadmium Sulfide Nanorods as a Novel p-n Heterojunction for Highly Efficient Visible-Light-Driven Hydrogen Production in Water

Cite this: DOI: 10.1039/xoxxoooooox

Received ooth January 2012,
Accepted ooth January 2012

DOI: 10.1039/xoxxoooooox

www.rsc.org/

Zijun Sun, Qiudi Yue, Jingshi Li, Jun Xu, Huafei Zheng, Pingwu Du*

Developing efficient photocatalysts made of earth-abundant elements for hydrogen (H_2) production from water is considered to be a key pathway for future clean energy supply. Herein we give the first report that p-type copper phosphide (Cu_3P) can be an efficient promoter to improve photocatalytic H_2 production from water when loaded on n-type cadmium sulphide nanorods (CdS NRs). The formation of a p-n junction in Cu_3P/CdS NRs leads to fast charge transfer and enhanced photocatalytic activity under visible light irradiation. Under optimal conditions, the H_2 evolution rate was as high as ~200 μmol h^{-1} mg^{-1} ($\lambda > 420$ nm) and the apparent quantum yield at $\lambda = 450$ nm was ~25% in water.

Due to serious environmental issues and the increasing clean energy demand, developing new energy sources to substitute for fossil fuels is an urgent priority. Hydrogen is considered to be an ideal energy carrier for a future clean energy supply system because of its high energy capacity and environmental friendliness.[1-2] Since the discovery of hydrogen production through the photoelectrochemical water splitting on TiO_2 in early 1970s,[3] photocatalytic hydrogen production from water over semiconductors has attracted much attention during the past few decades.[4-9] The main challenge for its commercial application is to produce hydrogen efficiently using photocatalysts that have long-term stability and low cost.[10-11] To achieve hydrogen production under visible light, the photocatalysts should have a proper band gap for visible light absorption and enough redox potential for water splitting.[12-13]

Among all the visible-light-responsive photocatalysts, n-type semiconductor CdS appears to be one of the most promising materials for photocatalytic H_2 evolution due to its high activity under visible light (narrow band gap, E_g ~2.4 eV) and sufficiently negative flat-band potential for proton reduction.[14-17] However, pure CdS is not very stable and exhibits low photocatalytic activity due to its fast electron-hole recombination and photocorrosion.[18] To solve these problems, several approaches have been applied to functionalize CdS semiconductor, such as loading an appropriate cocatalyst. Cocatalysts, which can effectively enhance the transfer of photogenerated charge carriers, play a very important role in promoting the photocatalytic activity.[19-21] The most common and effective cocatalyst is Pt,[15, 22] and other noble-metal-based materials, such as Ru and Pd,[23-24] are also studied as cocatalysts owing to the physicochemical properties being similar to Pt. Unfortunately, the high price and scare supply of noble metals limit their large-scale application. An alternative that has been studied is cocatalysts based on non-noble metals, such as Mo,[21, 25-27], Co,[19, 28-31], and Ni.[19, 32-33] Unhappily, the catalytic performances of these cocatalysts are generally worse than noble metals and therefore, it is necessary to develop more cost-effective and robust catalysts for H_2 production. Another approach to enhance the photocatalytic activity is to construct a p-n junction to retard the electron-hole recombination and improve the charge separation.

Cu_3P, as a p-type semiconductor, was previously reported for application in lithium ion batteries.[34-38] However, the use of Cu_3P for photocatalytic H_2 production has not received prior investigation. Herein we report the synthesis and evaluation of a novel and low-cost Cu_3P/CdS NRs p-n heterojunction photocatalyst for highly efficient H_2 production from water. Under optimal conditions, the H_2 evolution rate using this Cu_3P semiconductor was as high as ~200 μmol h^{-1} mg^{-1} ($\lambda > 420$ nm) and the apparent quantum yield was ~25% in water with Na_2S/Na_2SO_3 as the electron donors ($\lambda = 450$ nm). Furthermore, a photocatalytic mechanism based on the Cu_3P/CdS NRs p-n junction is proposed and discussed.

Cu_3P/CdS NRs were synthesized by a simple solvothermal method with the content ratio of Cu_3P at 0 % - 2.90 wt %. The as-prepared samples were labeled as CP1, CP2, CP3, and CP4, respectively. The copper ratio in each sample was measured by ICP-AES and the results are shown in Table S1. The Cu_3P ratios were calculated based on the copper contents.

Figure 1a shows the powder XRD patterns of CdS, Cu_3P/CdS, and Cu_3P. The Cu_3P/CdS and CdS samples show the peaks of 2θ at 24.8°, 26.5°, 28.2°, 36.7°, 43.7°, 47.9°, 51.9°, and 66.8°, which were

indexed to the (100), (002), (101), (102), (110), (103), (112), and (203) lattice fringe diffractions of hexagonal CdS (PDF#77-2306), respectively. For comparison, the Cu_3P shows peaks located at 36.0°, 39.0°, 41.5°, 45.1°, and 46.2°, which correspond respectively to the (112), (202), (211), (300), and (213) lattice diffractions of hexagonal Cu_3P (PDF#71-2261). After loading Cu_3P onto CdS, no obvious diffraction peaks belonging to Cu_3P were observed and all reflections showed no significant difference from CdS, which might result from the low content of Cu_3P in Cu_3P/CdS samples and high dispersion of Cu_3P nanomaterials deposited on the surface of CdS NRs.[16, 39-40] To identify the surface chemical composition and valence state of Cu_3P/CdS NRs, the XPS spectra were measured (Figure 1b). The survey scan shows the existence of Cd, S, Cu, and P elements. No other elements were observed except C element as the reference and O element from the absorbed gaseous molecules.

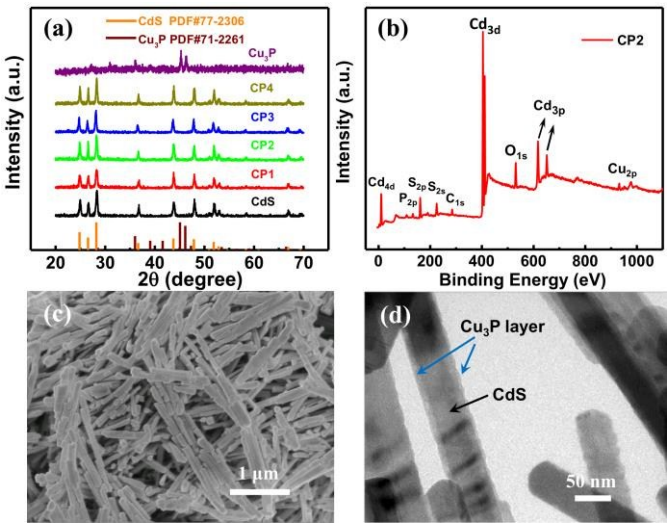

Figure 1. (a) Powder XRD patterns of Cu_3P/CdS samples containing different amount of Cu_3P. **(b)** XPS spectrum, **(c)** SEM image, **(d)** TEM image of CP2 sample.

Figure 1c shows a low-magnification SEM image of Cu_3P/CdS NRs (CP2 sample, Cu_3P 0.44 wt %) with the diameter of ca.40-90 nm and length from 0.4 μm to 2 μm. The SEM image of pure CdS NRs is shown in Figure S1a for comparison, as well as the SEM image of Cu_3P (Figure S1b). The slight increase of the diameter from CdS NRs to Cu_3P/CdS NRs suggests that Cu_3P has been successfully loaded on the CdS NRs. The TEM image shows an obvious core-shell structure of Cu_3P/CdS NRs with a thin layer Cu_3P (Figure 1d).

The HRTEM measurement can provide further insight into the crystalline morphologies and microstructural details of the core-shell nanostructure. Figure 2a shows the interfacial region of the Cu_3P/CdS NRs, demonstrating that Cu_3P nanoparticles were successfully loaded onto the surface of the single crystalline hexagonal CdS NRs. The crystalline planes for CdS can be recognized by the presence of the (002) lattice distance at 0.34 nm. Moreover, the lattice fringe distances of 0.22 nm and 0.25 nm can be assigned to the (211) and (112) planes of Cu_3P, respectively. These results suggest that Cu_3P nanoparticles are closely attached to the CdS nanorods, which could be highly beneficial to fast charge transfer between Cu_3P and CdS materials. In addition, the selected-area electron diffraction (SAED) analysis showed ordered diffraction spots, revealing the single crystalline nature of the CdS NRs (Figure 2b).

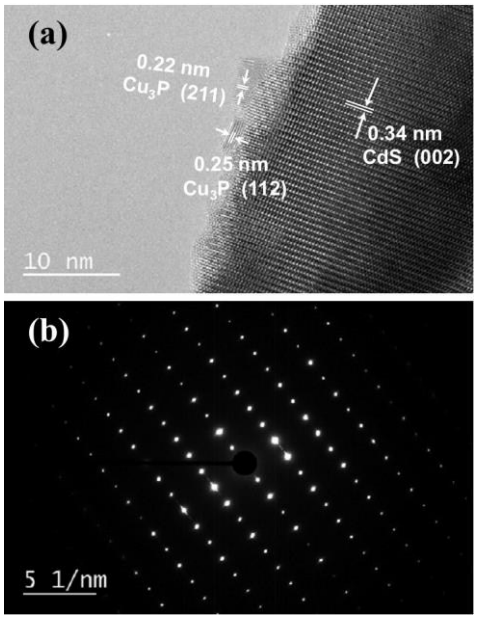

Figure 2. (a) HRTEM image, **(b)** Selected area electron diffraction (SAED) data of CP2 sample.

The EDX spectrum further confirmed the existence of Cd, S, Cu, and P, as shown in Figure 3a. Furthermore, the EDX elemental mapping images clearly show the distribution of Cd, S, Cu, and P elements (Figures 3b-3e). The observed Mo element is from the molybdenum grid substrate. The EDX mapping images of a single nanorod further reveal that both Cu and P elements are uniformly distributed in the whole nanorod. All these results clearly confirm the successful synthesis of core-shell Cu_3P/CdS NRs by a facile solvothermal method.

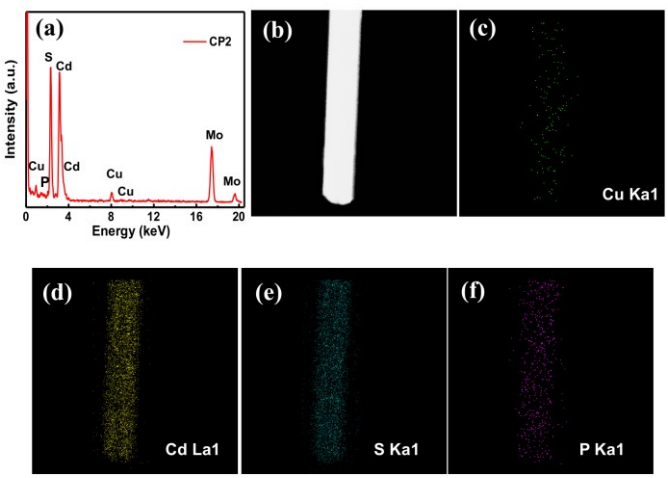

Figure 3. (a) EDX spectrum of CP2. EDX-mapping of CP2: **(b)** bright field image, **(c)** Cu element mapping, **(d)** Cd element mapping, **(e)** S element mapping, and **(f)** P element mapping.

Photocatalytic hydrogen production experiments were carried out using the as-prepared Cu_3P/CdS NRs photocatalysts in water under visible light irradiation ($\lambda > 420$ nm). The experimental set up is shown in scheme S1. Figure 4a shows the rate of H_2 evolution using

Cu_3P/CdS samples in the presence of Na_2S and Na_2SO_3 as the electron donors. It was found that an appropriate amount of Cu_3P can significantly enhance the photocatalytic activity for H_2 production in water. The rate of H_2 evolution initially increased and then decreased with increasing amounts of Cu_3P. With low content of Cu_3P loading (0.03 wt %) on CdS (CP1), the H_2 evolution rate was ~96 μmol h^{-1} mg^{-1}. The highest photocatalytic activity was achieved using CP2, presenting a H_2 evolution rate of ~184 μmol h^{-1} mg^{-1}. This phenomenon can be explained as follows: (1) excess Cu_3P covered on the CdS surface probably inhibit the incident light absorption by CdS and then decrease the photogenerated electrons from the CdS NRs; (2) excess Cu_3P could decrease the surface active sites of CdS.[21, 40-41] For comparison, in the absence of Cu_3P, CdS showed very low activity, having a H_2 evolution rate of only ~28 μmol h^{-1} mg^{-1}. Although the mechanical mixture of Cu_3P and CdS (0.44 wt % Cu_3P) showed a slightly higher rate than CdS (~40 μmol h^{-1} mg^{-1}), it is still much less than the Cu_3P/CdS samples prepared by the solvothermal method. In addition, the Cu_3P alone showed no appreciable H_2 production with visible light irradiation, revealing that Cu_3P is not an active photocatalyst.

The apparent quantum yield (φ) for photocatalytic H_2 production using CP2 photocatalyst was measured under 450 nm monochromatic light irradiation (Figure 4b). The result showed that the H_2 evolution rate reached ~88 μmol h^{-1} mg^{-1} with φ~25% after 8 hours of irradiation. The present efficient quantum yield from visible light energy into chemical energy indicated that Cu_3P/CdS NRs is a highly efficient photocatalyst.

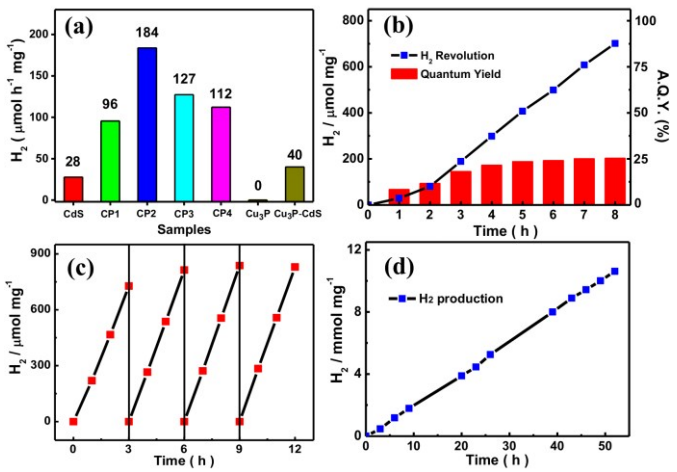

Figure 4. (a) Comparison of photocatalytic H_2 evolution rates of CdS, CP1, CP2, CP3, CP4, Cu_3P, and mixed Cu_3P-CdS samples at ambient temperature under visible light (λ > 420 nm). The system contains 1.0 mg photocatalyst, 0.75 M Na_2S, and 1.05 M Na_2SO_3 in 20 mL deionized water. **(b)** Time courses of H_2 production and apparent quantum yield on CP2 under monochromatic 450 nm (±5 nm) light irradiation using 1.0 mg photocatalyst in a 20 mL aqueous solution containing 1.25 M Na_2S and 1.75 M Na_2SO_3. **(c)** Cycling runs for photocatalytic hydrogen evolution in the presence of 1.0 mg CP2 photocatalyst in a 20 mL aqueous solution containing 1.25 M Na_2S and 1.75 M Na_2SO_3. After every 3 hours, the evolved H_2 was evacuated. **(d)** Long-term evolution of H_2 under visible light irradiation (λ > 420 nm) using CP2 photocatalyst. The system contains 1.0 mg photocatalyst, 1.25 M Na_2S, and 1.75 M Na_2SO_3 in 50 mL deionized water.

Besides its high activity, Cu_3P/CdS NRs material exhibits good stability during photocatalysis. The reaction system was evacuated to remove the evolved H_2 every 3 hours and the process was carried out repeatedly. As shown in Figure 4c, no significant decrease in the activity for photocatalytic H_2 production can be observed in 12 hours of cycling tests. Moreover, analysis of the photocatalytic efficiency after long-term operation was also performed, with the results shown in Figure 4d. After 50 hours of irradiation, a total of ~10 mmol H_2 was produced with a constant rate of ~200 μmol h^{-1} mg^{-1}. These results indicate the good stability of Cu_3P/CdS NRs for photocatalytic H_2 production under visible light. In addition, the SEM image of Cu_3P/CdS NRs had no significant change after photocatalysis. Figure S2 shows the SEM image of CP2 sample after 5 hours of irradiation. The image still has a rod-like structure, with nearly the same length and diameter as the sample before illumination, indicating that Cu_3P/CdS NRs material is a robust photocatalyst in the present photocatalytic H_2 evolution system.

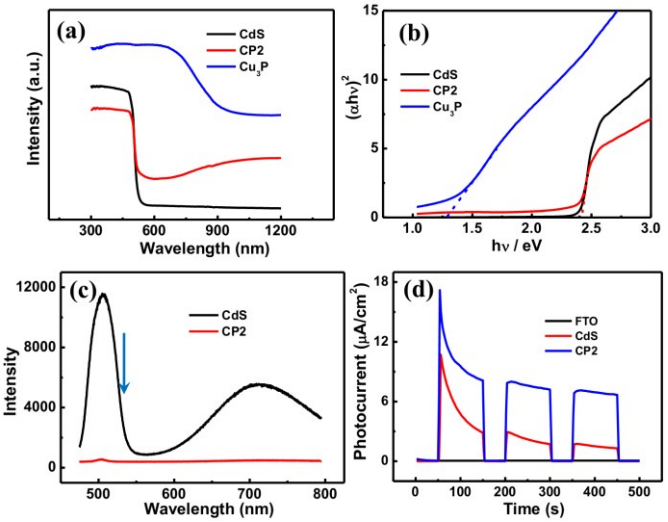

Figure 5. (a) The UV-vis diffuse reflectance spectra of and **(b)** the estimated band gap of the CdS, CP2, and Cu_3P. **(c)** The steady-state photoluminescence (PL) spectra of the CdS and CP2. **(d)** The transient photocurrent responses of blank FTO, CdS, and CP2.

The optical properties of the pure CdS, Cu_3P/CdS, and pure Cu_3P were measured by using a UV-vis-NIR spectrophotometer. Figure 5a shows the UV-vis absorption spectra for all samples. The spectrum of pure CdS displayed a sharp edge at around 530 nm. The optical band gap energy (Eg) is estimated to be about 2.4 eV by the Tauc plot (Figure 5b),[42] which agrees well with the reported value.[14, 43-44] The absorption onset of Cu_3P/CdS is also located at around 530 nm, probably originating from the absorption of CdS in Cu_3P/CdS heterojunction photocatalysts. The same absorption edges of pure CdS and Cu_3P/CdS indicated that copper did not dope into the CdS lattice in Cu_3P/CdS. The increased absorption features of Cu_3P/CdS in the region from 600 nm to 1200 nm should be ascribed to the contribution of Cu_3P. The pure Cu_3P shows the absorption edge at about 950 nm and the band gap energy (Eg) was estimated to be about 1.3 eV, which is consistent with the literature.[34]

In order to study the migration, transfer, and recombination processes of the photogenerated charge carriers over Cu_3P/CdS, the photoluminescence (PL) spectra were examined. Figure 5c shows the PL spectra of CdS and Cu_3P/CdS under excitation at 405 nm. It was observed that the as-prepared CdS displayed two distinct emission band at ~511 nm and ~713 nm, which is in agreement with previous studies.[45-46] The broad photoluminescence spectrum centered at ~713

nm should be the trapped emission, which was mainly due to the surface defects.[47-48] Such surface defects would act as recombination centers for electron-hole pairs to lower the photocatalytic activity. The PL spectrum of Cu_3P/CdS was similar to that of CdS. However, the emission intensity was much weaker than that of CdS, indicating the transfer of photogenerated charge carriers in Cu_3P/CdS by forming p-n interfacial junctions.[49]

To further investigate the photocatalytic H_2 production mechanism over Cu_3P/CdS, photocurrent tests were performed. As shown in Figure 5d, the Cu_3P/CdS photocatalyst exhibits much higher photocurrent response than CdS NRs, revealing that the charge transfer process in Cu_3P/CdS is more effective than pure CdS. The fast transfer of charge carriers can highly enhance photocatalytic activity for H_2 production according to the literature.[19, 27, 50]

Based on above results, a possible reaction mechanism for photocatalytic H_2 evolution using Cu_3P/CdS heterojunction is proposed and the schematic diagram is illustrated in Scheme 1. Both Cu_3P and CdS can absorb visible light to produce photoinduced electron-hole pairs. Since Cu_3P is a p-type semiconductor[34] and CdS is an n-type material,[12] a large number of nanoscale p-n junctions could be generated when two such types of semiconductor materials are closely attached. It has been reported that the conduction band (CB) position of CdS (~-3.98 eV vs. AVS[51]) is lower than that of Cu_3P (~-3.8 eV vs. AVS[34]). Therefore, the photoinduced electrons on the CB of Cu_3P can directly transfer to the CB of CdS. The electrons, together with the electrons excited from the VB of CdS, would transfer to the surface of CdS to reduce H^+ for H_2 production. As for the valence band (VB), the corresponding VB position of CdS (~-6.38 eV vs. AVS) is also lower than that of Cu_3P (~-5.1 eV vs. AVS). As a result, the photogenerated holes on the VB of CdS can migrate to the VB of Cu_3P, which will greatly reduce the recombination process of electron-hole pairs and further lead to enhanced stability of the CdS and an improved H_2 evolution rate. Therefore, efficient charge separation was successfully achieved by the nanoscale p-n junctions in Cu_3P/CdS. The close contact between CdS and Cu_3P could facilitate the charge transfer, which would improve the photocatalytic H_2 evolution activity and stability.

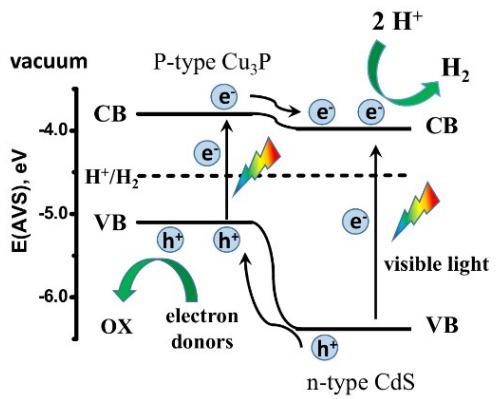

Scheme 1. A possible reaction mechanism for photocatalytic H_2 evolution using the Cu_3P/CdS heterojunction.

Conclusions

In conclusion, Cu_3P/CdS NRs core-shell heterostructures were successfully constructed by in situ deposition of Cu_3P onto CdS through a facile solvothermal method. Cu_3P nanomaterials were tightly attached to the surface of CdS, leading to the formation of p-n junctions between p-type Cu_3P and n-type CdS. The p-n junctions in Cu_3P/CdS can promote fast charge transfer and reduce charge recombination. Under optimal conditions, the Cu_3P/CdS exhibited a H_2 evolution rate of ~200 $\mu mol \cdot h^{-1} \cdot mg^{-1}$ with a maximum apparent quantum yield of ~25% when excited at 450 nm. The photocatalytic results indicate that Cu_3P is a highly active promoter when loaded on CdS to form p-n junctions for H_2 production. This work not only supports the possibility of using cost-effective p-type Cu_3P for photocatalytic H_2 production but also shows that a proper p-n junction structure is crucial for high photocatalytic activity in a hybrid photocatalyst.

Acknowledgements

This work was financially supported by NSFC (21271166, 21473170), the Fundamental Research Funds for the Central Universities (WK3430000001, WK2060140015, WK2060190026), the Program for New Century Excellent Talents in University (NCET), and the Thousand Young Talents Program.

Notes and references

[a] *Key Laboratory of Materials for Energy Conversion, Chinese Academy of Sciences, Department of Materials Science and Engineering, iChEM (Collaborative Innovation Center of Chemistry for Energy Materials), University of Science and Technology of China, 96 Jinzhai Road, Hefei, Anhui Province, 230026, P. R. China. Fax: 86-551-63606207; E-mail: dupingwu@ustc.edu.cn*

† Electronic Supplementary Information (ESI) available: Experimental details, ICP-AES data of copper in Cu_3P/CdS NRs, SEM images of CdS and Cu_3P, and SEM image of Cu_3P/CdS after 5 hours of visible light irradiation. See DOI: 10.1039/c000000x/

1 H. B. Gray, *Nat. Chem.* 2009, ***1***, 7-7.
2 N. S. Lewis, D. G. Nocera, *Proc. Natl. Acad. Sci. U. S. A.* 2006, ***103***, 15729-15735.
3 A. Fujishima, K. Honda, *Nature* 1972, ***238***, 37-38.
4 E. Elmalem, A. E. Saunders, R. Costi, A. Salant, U. Banin, *Adv. Mater.* 2008, ***20***, 4312-4317.
5 M. Hara, T. Kondo, M. Komoda, S. Ikeda, K. Shinohara, A. Tanaka, J. N. Kondo, K. Domen, *Chem. Commun.* 1998, 357-358.
6 R. Konta, T. Ishii, H. Kato, A. Kudo, *J. Phys. Chem. B* 2004, ***108***, 8992-8995.
7 A. Kudo, H. Kato, *Chem. Phys. Lett.* 2000, ***331***, 373-377.
8 J. Wang, D. N. Tafen, J. P. Lewis, Z. L. Hong, A. Manivannan, M. J. Zhi, M. Li, N. Q. Wu, *J. Am. Chem. Soc.* 2009, ***131***, 12290-12297.
9 M. Wang, J. Ioccozia, L. Sun, C. Lin, Z. Lin, *Energ Environ Sci* 2014, ***7***, 2182-2202.
10 A. J. Bard, M. A. Fox, *Acc. Chem. Res.* 1995, ***28***, 141-145.
11 D. G. Nocera, *Acc. Chem. Res.* 2012, ***45***, 767-776.
12 X. B. Chen, S. H. Shen, L. J. Guo, S. S. Mao, *Chem. Rev.* 2010, ***110***, 6503-6570.
13 Y. Ma, X. L. Wang, Y. S. Jia, X. B. Chen, H. X. Han, C. Li, *Chem. Rev.* 2014, ***114***, 9987-10043.
14 M. Matsumura, S. Furukawa, Y. Saho, H. Tsubomura, *J. Phys. Chem.* 1985, ***89***, 1327-1329.
15 H. J. Yan, J. H. Yang, G. J. Ma, G. P. Wu, X. Zong, Z. B. Lei, J. Y. Shi, C. Li, *J. Catal.* 2009, ***266***, 165-168.

16 X. Zong, G. P. Wu, H. J. Yan, G. J. Ma, J. Y. Shi, F. Y. Wen, L. Wang, C. Li, *J. Phys. Chem. C* 2010, ***114***, 1963-1968.
17 J. H. Yang, H. J. Yan, X. L. Wang, F. Y. Wen, Z. J. Wang, D. Y. Fan, J. Y. Shi, C. Li, *J. Catal.* 2012, ***290***, 151-157.
18 N. Bao, L. Shen, T. Takata, K. Domen, A. Gupta, K. Yanagisawa, C. A. Grimes, *J. Phys. Chem. C* 2007, ***111***, 17527-17534.
19 Z. P. Yan, X. X. Yu, A. L. Han, P. Xu, P. W. Du, *J. Phys. Chem. C* 2014, ***118***, 22896-22903.
20 Z. P. Yan, H. T. Wu, A. Han, X. X. Yu, P. W. Du, *Int. J. Hydrogen Energy* 2014, ***39***, 13353-13360.
21 X. Zong, H. J. Yan, G. P. Wu, G. J. Ma, F. Y. Wen, L. Wang, C. Li, *J. Am. Chem. Soc.* 2008, ***130***, 7176-7177.
22 J. G. Yu, L. F. Qi, M. Jaroniec, *J. Phys. Chem. C* 2010, ***114***, 13118-13125.
23 J. Sato, N. Saito, Y. Yamada, K. Maeda, T. Takata, J. N. Kondo, M. Hara, H. Kobayashi, K. Domen, Y. Inoue, *J. Am. Chem. Soc.* 2005, ***127***, 4150-4151.
24 T. Sreethawong, S. Yoshikawa, *Catal. Commun.* 2005, ***6***, 661-668.
25 B. L. Zhu, B. Z. Lin, Y. Zhou, P. Sun, Q. R. Yao, Y. L. Chen, B. F. Gao, *J. Mater. Chem. A* 2014, ***2***, 3819-3827.
26 J. J. Wang, Z. Y. Guan, J. Huang, Q. X. Li, J. L. Yang, *J. Mater. Chem. A* 2014, ***2***, 7960-7966.
27 Y. L. Min, G. Q. He, Q. J. Xu, Y. C. Chen, *J. Mater. Chem. A* 2014, ***2***, 2578-2584.
28 P. Du, R. Eisenberg, *Energy Environ. Sci.* 2012, ***5***, 6012-6021.
29 Z. J. Li, X. B. Li, J. J. Wang, S. Yu, C. B. Li, C. H. Tung, L. Z. Wu, *Energy Environ. Sci.* 2013, ***6***, 465-469.
30 W. R. McNamara, Z. Han, C.-J. Yin, W. W. Brennessel, P. L. Holland, R. Eisenberg, *Proc. Natl. Acad. Sci. U. S. A.* 2012, ***109***, 15594-15599.
31 W. R. McNamara, Z. Han, P. J. Alperin, W. W. Brennessel, P. L. Holland, R. Eisenberg, *J. Am. Chem. Soc.* 2011, ***133***, 15368-15371.
32 T. Y. Peng, X. H. Zhang, P. Zeng, K. Li, X. G. Zhang, X. G. Li, *J. Catal.* 2013, ***303***, 156-163.
33 Z. Khan, M. Khannam, N. Vinothkumar, M. De, M. Qureshi, *J. Mater. Chem.* 2012, ***22***, 12090-12095.
34 G. Manna, R. Bose, N. Pradhan, *Angew. Chem. Int. Ed.* 2013, ***52***, 6762-6766.
35 H. Pfeiffer, F. Tancret, M. P. Bichat, L. Monconduit, F. Favier, T. Brousse, *Electrochem. Commun.* 2004, ***6***, 263-267.
36 O. Crosnier, L. F. Nazar, *Electrochem. Solid-State Lett.* 2004, ***7***, A187-A189.
37 M. P. Bichat, T. Politova, J. L. Pascal, F. Favier, L. Monconduit, *J. Electrochem. Soc.* 2004, ***151***, A2074-A2081.
38 M. P. Bichat, T. Politova, H. Pfeiffer, F. Tancret, L. Monconduit, J. L. Pascal, T. Brousse, F. Favier, *J. Power Sources* 2004, ***136***, 80-87.
39 Y. B. Chen, Z. X. Qin, X. X. Wang, X. Guo, L. J. Guo, *RSC Adv.* 2015, ***5***, 18159-18166.
40 J. Zhang, S. Z. Qiao, L. F. Qi, J. G. Yu, *Phys. Chem. Chem. Phys.* 2013, ***15***, 12088-12094.
41 J. G. Hou, C. Yang, Z. Wang, S. Q. Jiao, H. M. Zhu, *Rsc Adv* 2012, ***2***, 10330-10336.
42 J. Tauc, Grigorov.R, A. Vancu, *Phys. Status Solidi* 1966, ***15***, 627-637.
43 J. F. Reber, M. Rusek, *J. Phys. Chem.* 1986, ***90***, 824-834.
44 L. A. Silva, S. Y. Ryu, J. Choi, W. Choi, M. R. Hoffmann, *J. Phys. Chem. C* 2008, ***112***, 12069-12073.
45 S. Q. Liu, Z. Chen, N. Zhang, Z. R. Tang, Y. J. Xu, *J. Phys. Chem. C* 2013, ***117***, 8251-8261.
46 D. Xu, Z. P. Liu, J. B. Liang, Y. T. Qian, *J. Phys. Chem. B* 2005, ***109***, 14344-14349.
47 Y. B. Chen, Z. X. Qin, X. X. Wang, X. Guo, L. J. Guo, *RSC Adv.* 2015, ***5***, 18159-18166.
48 Y. W. Wang, G. W. Meng, L. D. Zhang, C. H. Liang, J. Zhang, *Chem. Mater.* 2002, ***14***, 1773-1777.
49 J. G. Radich, N. R. Peeples, P. K. Santra, P. V. Kamat, *J. Phys. Chem. C* 2014, ***118***, 16463-16471.
50 Y. B. Xie, *Adv. Funct. Mater.* 2006, ***16***, 1823-1831.
51 Y. Xu, M. A. A. Schoonen, *Am. Mineral.* 2000, ***85***, 543-556.

TOC Figure

The present study shows that p-type copper phosphide (Cu_3P) can be an efficient promoter to improve photocatalytic H_2 production from water when loaded on n-type cadmium sulphide nanorods.